ELECTRON SCATTERING FROM A TENSOR-POLARIZED DEUTERIUM INTERNAL TARGET AT NIKHEF.

J. F. J. van den Brand,[2,3,6]

for the

91-12 COLLABORATION

M. Ferro-Luzzi,[1] M. Bouwhuis,[2] E. Passchier,[2] Z.-L. Zhou,[3] R. Alarcon,[4] M. Anghinolfi,[5] R. van Bommel,[2] T. Botto,[2] J. F. J. van den Brand,[2,3,6] M. Buchholz,[3] H.J. Bulten,[3] S. Choi,[4] J. Comfort,[4] S. Dolfini,[4] R. Ent,[7] C. Gaulard,[4] D. Higinbotham,[8] C. W. de Jager,[2] E. P. van Klaveren,[2] E. Konstantinov,[9] J. Lang,[1] D. J. de Lange,[2] M. A. Miller,[3] D. Nikolenko,[9] G. J. Nooren,[2] N. Papadakis,[2] I. Passchier,[2] H. R. Poolman,[2] S. G. Popov,[9] I. Rachek,[9] M. Ripani,[5] E. Six,[4] J. J. M. Steijger,[2] M. Taiuti,[5] O. Unal,[3] N. Vodanis,[2] H. de Vries.[2]

[1] *Institut für Teilchenphysik, Eidg. Technische Hochschule, CH-8093 Zürich, Switzerland*

[2] *NIKHEF, P.O. Box 41882, 1009 DB Amsterdam, The Netherlands*

[3] *Department of Physics, University of Wisconsin, Madison, Wisconsin 53706, USA*

[4] *Department of Physics, Arizona State University, Tempe, AZ 85287, USA*

[5] *Istituto Nazionale di Fisica Nucleare (INFN), I-16146 Genova, Italy*

[6] *Department of Physics and Astronomy, Vrije Universiteit, Amsterdam, The Netherlands*

[7] *CEBAF, Newport News, VA 23606, and Department of Physics, Hampton University, Hampton, VA 23668, USA*

[8] *Department of Physics, University of Virginia, Charlottesville, VA 22901, USA*

[9] *Budker Institute for Nuclear Physics, Novosibirsk, 630090 Russian Federation*

We report on measurements with a polarized deuterium target internal to the NIKHEF electron storage ring. The target and polarimetry techniques are described. Results are given for an absolute measurement of the tensor analyzing powers T_{20} and T_{22} in elastic electron-deuteron scattering at momentum transfer of 1.6 fm^{-1}. The techniques demonstrated have broad applicability to further measurements of spin-dependent electron scattering.

1. Introduction

Measurements of spin-dependent electron scattering have the potential to enhance our understanding of nucleon and nuclear structure. For example, spin observables in elastic, quasi-elastic, and deep-inelastic scattering from polarized deuterium are predicted to provide important information on the effects of D-wave components in the ground state of ^{2}H, the largely unknown charge form factor of the neutron, and the neutron spin structure functions. This has prompted development of both polarized ^{2}H targets for use with internal [1] or external beams [2] and polarimeters for measuring the polarization of recoiling hadrons [3]. Indeed the first round of measurements of spin-dependent e-^{2}H scattering has been carried out at Novosibirsk [4,5], Bonn [6], MIT-Bates [7,8], and SLAC [9].

Polarized internal gas targets in electron storage rings have the advantage that spin-dependent scattering from chemically and isotopically pure atomic species of high polarization can be realized. They offer rapid polarization reversal and flexible orientation of the nuclear spin direction by using low magnetic holding fields, a low thickness at high luminosity which allows for the detection of low-energy recoiling hadrons, and access to a broad kinematic range by using large acceptance detectors. For polarized deuterium one has the additional ability to reverse the tensor polarization, P_{zz}, at fixed vector polarization, P_z, and vice versa. Consequently, small systematic errors can be expected.

Since the physics issues in polarized elastic electron-deuteron scattering are well known, we restrict the discussion in section 2. to an overview of the target setup and the polarimetry techniques. The tensor analyzing powers T_{20} and T_{22} for elastic electron-deuteron scattering were measured at a momentum transfer of 1.6 fm^{-1} and the data are presented in section 3..

2. Tensor-Polarized Deuterium Target and Polarimetry

An overview of the experiment is given in Fig. 1. The deuterium target is located internal to the AmPS electron ring at NIKHEF. Nuclear-polarized deuterium gas is provided by an atomic beam source (ABS). This source consists of an RF-dissociator, a cooled nozzle, two sextupole electromagnets and two RF transition units[10]. The sextupole magnets focus, according to the Stern-Gerlach principle, atoms with electron spin up (states 1,2,3) and reject the states with spin down (4,5,6). A medium field unit induces a 1-4 transition, while a strong field unit induces either a 3-5 transition or a 2-6 transition, resulting in a tensor polarization of -2 or +1, respectively.

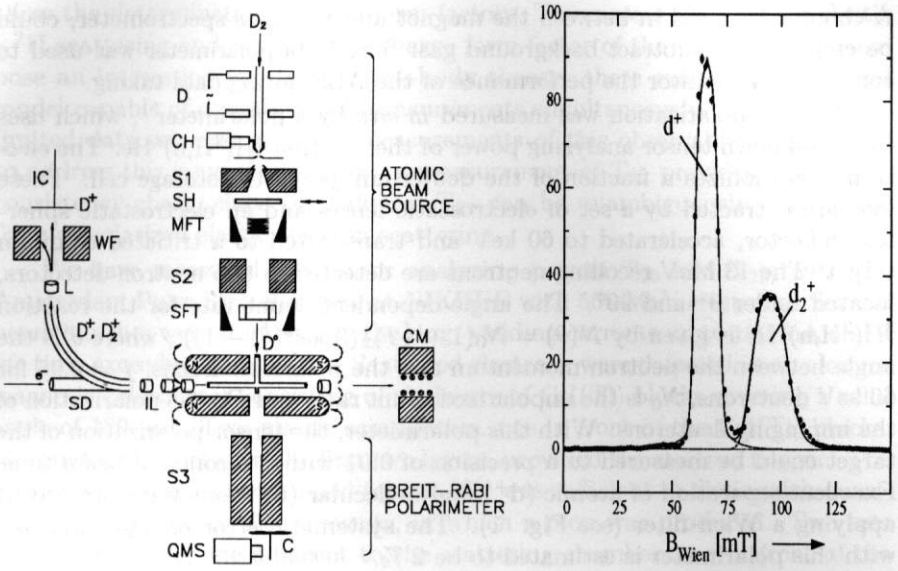

Figure 1: Left panel: Schematic outline of the atomic beam source, Breit-Rabi polarimeter, internal target and ion extraction system. All components, except the target holding field and the compensation magnet, are in the vacuum. D: RF-dissociator; CH: coldhead; S1,S2,S3: sextupole magnets; SH: shutter; MFT (SFT) medium (strong) field transition unit; IL: ion extraction lenses; SD: spherical deflector; WF: Wien filter; IC: ion collector; QMS: quadrupole mass spectrometer; C: chopper. Right panel: Ion current (nA) as a function of magnetic field in the Wien filter. The curves represent fits to the data.

The atomic beam from the ABS is injected into a T-shaped conductance limiter. In this way the atomic density is increased by two orders of magnitude compared to a free atomic beam. This so-called storage cell was cooled to 150 K to further increase the target density and polarization. The cell has been constructed from ultra-pure aluminum with a thickness of 25 μm. In order to minimize recombination and depolarization, it has been coated with a solution of PTFE3170 liquid Teflon in water. The storage cell (feed tube) has dimensions of 400 mm (130 mm) in length and 15 mm (12 mm) in diameter. Presently we obtain with this geometry a target thickness (viewed by the detectors) of 2×10^{13} at/cm^2. A small sample tube (4 mm diameter) is located opposite to the feed tube, and allows to extract a fraction (about 10%) of the injected gas for subsequent analysis by a Rabi polarimeter. This polarimeter consists of a 41 cm long permanent tapered sextupole magnet (entrance (exit) radius 3 mm (1.5 mm), tip field about 0.44 T) in front of a quadrupole mass spectrometer.

A chopper, located in between the magnet and the mass spectrometer, could be employed to subtract background gas. The Rabi polarimeter was used to continuously monitor the performance of the ABS during data taking.

Nuclear polarization was measured *in situ* by a polarimeter[11], which uses the well-known tensor analyzing power of the reaction ^{3}H(^{2}H,n)^{4}He. The electron beam ionizes a fraction of the deuterium gas in the storage cell. These ions are extracted by a set of electrostatic lenses and an electrostatic spherical deflector, accelerated to 60 keV and transported to a tritiated titanium target. The 13 MeV recoiling neutrons are detected in two neutron detectors, located under 0° and 90°. The angle-dependent count rate for the reaction ^{3}H(^{2}H,n)^{4}He is given by $N(\theta) = N_0(1 + \frac{f}{4}P_{zz}(3\cos^2(\theta) - 1))$, where θ is the angle between the neutron momentum and the polarization axis, $f = 0.95$ for 60 keV deuterons, N_0 is the unpolarized count rate, and P_{zz} the polarization of the impinging deuterons. With this polarimeter, the tensor polarization of the target could be measured to a precision of 0.01 within seconds of beam time. Excellent separation of atomic (d^+) and molecular (d_2^+) ions was obtained by applying a Wien filter (see Fig. 1). The systematic error on P_{zz} measured with this polarimeter is estimated to be 2 %.

With the tritium polarimeter we measured the nuclear polarization of the *atoms* ($P_{zz}^+(D^+) = +0.664 \pm 0.019 \pm 0.017$ and $P_{zz}^-(D^+) = -1.215 \pm 0.036 \pm 0.023$). The target contains also molecules originating from imperfect dissociation, residual gas in the target chamber and ABS, and from recombination on the cell walls. We accurately determined the atomic fraction, by performing Wien scans of the ion current as a function of the magnetic field and by alternating between data from the ABS and from a buffer vessel, in which we could prepare arbitrary mixtures of deuterium (mass 4) and hydrogen (mass 2). The atomic fraction, $\eta = \frac{t_{D^+}}{t_{D^+} + 2t_{D_2^+}}$ where t_i is the areal target thickness of the species, amounted to $\eta = 0.71 \pm 0.02$. Furthermore, the flexibility of our setup enabled us to study depolarization effects due to the spin-exchange mechanism, and due to electron-beam induced hyperfine transitions. We also found that the recombined molecules do retain part of the atomic polarization ($P_{zz}(D_2^+) = 0.81 \pm 0.33$). These issues are relevant for future measurements in the field (e.g. HERMES at DESY).

3. Tensor Analyzing Powers for Elastic e-d Scattering

Elastic electron scattering from the deuteron is completely described by the G_C, G_Q, and G_M form factors. Cross section measurements yield the structure functions A(G_C,G_Q,G_M) and B(G_M), which combined with T_{20}(G_C,G_Q,G_M)

allow the determination of these form factors. The present data set for elastic e-^{2}H scattering and the isoscalar charge form factor of the three-body system pose an interesting puzzle[12] for few-body theory: there exists *no* theoretical model capable of describing all measurements simultaneously. T_{20} has only a limited data set, and accurate measurements of this observable are required to address this issue. In addition, a measurement of T_{22} provides a stringent consistency check, since the value of T_{22} can be unambiguously determined from unpolarized elastic electron scattering.

We have measured the tensor analyzing powers T_{20} and T_{22}, with the Amsterdam Pulse Stretcher ring at NIKHEF with 565 MeV electrons. Several beam bunches were stacked into the ring, yielding currents up to 120 mA and a life time exceeding 15 minutes. Scattered electrons were detected in an electromagnetic calorimeter consisting of six layers of CsI(Tl) blocks covering a solid angle of 180 msr. Two plastic scintillators, one in front of the CsI(Tl) blocks, one sandwiched between the first two layers, provided the electron trigger. The total energy resolution obtained (about 8%) was sufficient to distinguish quasi-elastic events from inelastic events, in which a pion was produced. Two sets of wire chambers, one adjacent to the scattering chamber, one in front of the first trigger scintillator, were used for track reconstruction. The central angle of the electron detector was positioned at 35°. This resulted in a coverage in four-momentum transfer between $1.3 < q < 2.1$ fm^{-1} with a cross section and acceptance weighted average of $\bar{q} = 1.58$ fm^{-1}. The recoil deuterons were detected in a range telescope, consisting of 15 layers of 1 cm thick plastic scintillator preceded by 1 layer of 2 mm thickness. The detector was positioned at a central angle of 80°, and covered a solid angle of nearly 300 msr. The range telescope was preceded by two sets of wire chambers for track reconstruction. The minimum energy of the detected deuterons was 19 MeV. The left panel in Fig. 2 shows a time difference spectrum between electrons and hadrons for the event sample with and without cuts on angular correlations. It is seen that an unambiguous separation of the deuterons from protons was obtained by differences in time-of-flight, in energy loss in the scintillators, and by requiring kinematic correlations between electron and deuteron events. The right panel in Fig. 2 shows the reconstructed vertex distribution along the storage cell for ^{2}H(e,e'd) events. The expected triangular density distribution of the gas is observed, as illustrated by the curve obtained with a Monte Carlo technique. We also included in Fig. 2 the results from a run without gas flow from the ABS, established by inserting a shutter (shaded histogram). This unpolarized background amounts to 4% and was taken into account in the polarization determination.

The asymmetry $A = \sqrt{2}\frac{N^+ - N^-}{N^- \cdot P^+_{zz} - N^+ \cdot P^-_{zz}}$ was determined, where N^+ (N^-)

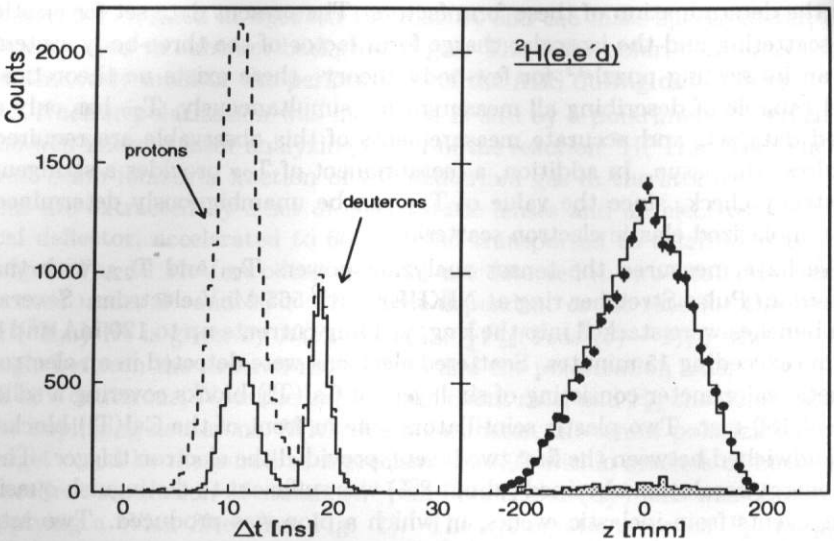

Figure 2: Left panel: time difference between electron and hadron for the event sample with (solid histogram) and without (dashed histogram) cuts on angular correlations. Right panel: reconstructed vertex position along the beam axis for the reaction ^{2}H(e,e'd). Both measurements with injected atomic beam (circles) and empty storage cell (shaded histogram) are shown. The curve indicates the Monte Carlo prediction.

corresponds to the number of events measured for P_{zz}^{+} (P_{zz}^{-}). The target spin vector was directed approximately parallel or perpendicular to the momentum transfer. The average spin angle was optimized for quasi-free scattering kinematics, resulting for elastic scattering in $\bar{\theta}_{\parallel}^{*} = 15°$ and $\bar{\theta}_{\perp}^{*} = 89°$. We found $A_{\parallel} = -0.317 \pm 0.028$ and $A_{\perp} = 0.210 \pm 0.019$. Since the spin dependent cross section is dominated by T_{20}, we expect the asymmetry to follow the spin-angular dependence of the associated Legendre function $P_2^0 = \frac{1}{2}(3\cos^2\theta^* - 1)$. The predicted change of sign in the tensor asymmetry is clearly observed when changing the spin angle. As a check on false asymmetries, we measured the asymmetry for unpolarized target gas and obtained $A_{unp} = 0.000 \pm 0.014$.

The 7% systematic error in T_{20} includes the uncertainties from the polarization measurement (6.6%) and the spin orientation angles (1.9%). Also included is the uncertainty from the correction for the small T_{21} and T_{22} contributions, which amounts to 0.7% and has been estimated from the existing data for $G_Q(Q^2)$ and $B(Q^2)$. The data for the two spin orientations also allow to extract T_{22}, resulting in $< T_{22} >= 0.022 \pm 0.019 \pm 0.003$. In Fig. 3 we compare the data for T_{20} and T_{22} with the results of other measurements and several state-of-the-art models [13,14,15,16,17].

We have included the results of experiments measuring T_{20} and T_{22} through

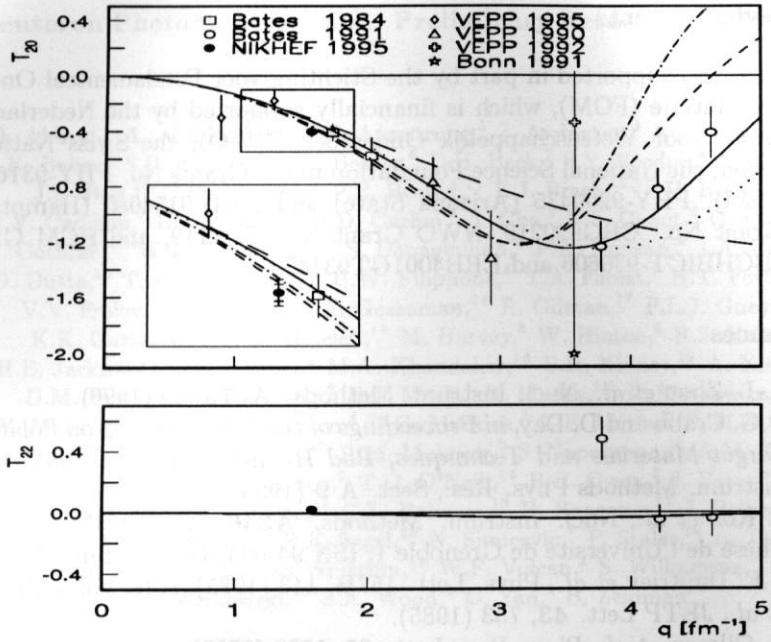

Figure 3: Data and theoretical predictions for T_{20} and T_{22}, as a function of momentum transfer. The curves represent various theoretical models: short-dashed for the NRIA including MEC from Ref. [13] by using the Argonne V14 potential; solid from Ref. [14] for the RIA including $\rho\pi\gamma$ and $\omega\sigma\gamma$ contributions; dotted for the RIA from Ref. [15] by using the Bonn Q potential; dot-dashed for the coupled-channels calculation of Ref. [16] for IA + MEC and model D'; long-dashed for the PQCD prediction of Ref. [17]. The inset shows the results in the q (T_{20}) range from 1.05 fm^{-1} (-0.55) to 1.90 fm^{-1} (-0.10). The heavy curve in the left bottom figure represents T_{22} calculated from a fit to the world data for $B(Q^2)$.

the recoil polarization technique [7,8]. The variation in theoretical predictions for T_{20} shows that precise measurements up to $q = 4$ fm^{-1} can distinguish between the various models shown. The experimental techniques established here are sufficient to obtain such data, with small statistical and systematic uncertainties, within a reasonable time frame.

Presently, we are upgrading both the ABS (by installing stronger sextupole magnets) and the electron storage ring (a smaller β function at the target region will enable the use of a cell with a smaller diameter. Furthermore, polarized electrons will be available in the fall of 1996). These modifications will allow us to measure polarization observables for hydrogen, deuterium, and ^{3}He with high precision. For example, we intend to measure T_{20} up to a momentum transfer of about 4 fm^{-1} in the spring of 1997.

Acknowledgements

This work was supported in part by the Stichting voor Fundamenteel Onderzoek der Materie (FOM), which is financially supported by the Nederlandse Organisatie voor Wetenschappelijk Onderzoek (NWO), the Swiss National Foundation, the National Science Foundation under Grants No. PHY-9316221 (Wisconsin), PHY-9200435 (Arizona State) and HRD-9154080 (Hampton), Nato Grant No. CRG920219, NWO Grant No. 713-119, and HCM Grant No ERBCHBICT-930606 and ERB4001GT931472.

References

1. Z.-L. Zhou *et al.*, Nucl. Instrum. Methods. **A378**, 40 (1996).
2. D.G. Crabb and D. Day, in *Proceedings of the 7th Workshop on Polarized Target Materials and Techniques, Bad Honnef, Germany, 1994* [Nucl. Instrum. Methods Phys. Res., Sect. A **9** (1995)].
3. S. Kox *et al.*, Nucl. Instrum. Methods. **A346**, 527 (1994); J.S. Réal, Thèse de l'Université de Grenoble 1, ISN 94-003, 1994, unpublished;
4. V.F. Dmitriev *et al.*, Phys. Lett. 157**B**, 143 (1985); B.B. Voitsekhovskii *et al.*, JETP Lett. **43**, 733 (1985).
5. R. Gilman *et al.*, Phys. Rev. Lett. **65**, 1733 (1990).
6. B. Boden *et al.*, Z. Phys. **C49**, 175 (1991).
7. M.E. Schulze *et al.*, Phys. Rev. Lett. **52**, 597 (1984).
8. I. The *et al.*, Phys. Rev. Lett. **67**, 173 (1991); M. Garçon *et al.*, Phys. Rev. C **49**, 2516 (1994).
9. K. Abe *et al.*, Phys. Rev. Lett. **75**, 25 (1995).
10. M. Ferro-Luzzi, Z.-L. Zhou, H.J. Bulten and J.F.J. van den Brand, Nucl. Instrum. Methods **A364**, 44 (1995).
11. Z.-L. Zhou, M. Ferro-Luzzi, J.F.J. van den Brand, H. J. Bulten *et al.*, accepted for publication in Nucl. Inst. Meth. **A** (June 1996).
12. H. Henning, J. Adam, Jr., P.U. Sauer, and A. Stadler, Phys. Rev. **C52**, R471 (1995).
13. R. Schiavilla and D.O. Riska, Phys. Rev. C **43**, 437 (1990).
14. E. Hummel and J.A. Tjon, Phys. Rev. C **42**, 423 (1990).
15. P.L. Chung, F. Coester, B.D. Keister, and W.N. Polyzou, Phys. Rev. C **37**, 2000 (1988).
16. P.G. Blunden, W.R. Greenberg, and E.L. Lomon, Phys. Rev. C **40**, 1541 (1989).
17. C.E. Carlson, Nucl. Phys. **A508**, 481c (1990).

Tensor Asymmetries Measured With The $^2\vec{\vec{H}}(e,e'p)$ Reaction

Z.-L. Zhou[1], M. Bouwhuis[2], M. Ferro-Luzzi[3], E. Passchier[2], R. Alarcon[4], M. Anghinolfi[5], R. van Bommel[2], T. Botto[2], J.F.J. van den Brand[1], M. Buchholz[1], H.J. Bulten[1], S. Choi[4], J. Comfort[4], S. Dolfini[4], R. Ent[6], C. Gaulard[4], D. Higinbotham[7], C.W. de Jager[2], E.P. van Klaveren[2], E. Konstantinov[8], J. Lang[3], D.J. de Lange[2], M.A. Miller[1], D. Nikolenko[8], G.J. Nooren[2], N. Papadakis[2], I. Passchier[2], H.R. Poolman[2], S.G. Popov[8], I. Rachek[8], M. Ripani[5], E. Six[4], J. Steijger[2], M. Taiuti[5], O. Unal[1], N. Vodinas[2], H. de Vries[2]

[1] *UW-Madison,* [2] *NIKHEF,* [3] *ETH,* [4] *ASU,* [5] *Genova,* [6] *TJNAF,* [7] *UVA,* [8] *Novosibirsk*

Tensor asymmetries for quasi-free $(e,e'p)$ scattering have been measured at NIKHEF using the medium-energy AmPS electron storage/stretcher ring and an internal target [1]. A large acceptance non-magnetic detector system was used to detect electrons in coincidence with protons or deuterons [2]. Data have been taken at a beam energy of 565 MeV, with beam currents up to 125 mA and an average luminosity of 10^{31} atoms/cm^{2}s, and with the target spin directed parallel and perpendicular to the momentum transfer. The target polarization was determined on-line during data taking through ion-extraction polarimetry [3]. Kinematics were selected with four-momentum transfers in the range $0.1 < Q^2 < 0.3$ (GeV/c)^2 and missing momenta up to 200 MeV/c.

The tensor asymmetries are presented as a function of θ_{np} (Fig. 1a and 1b) and ϕ_{np}(Fig. 1c and 1d), the angles of the knocked-out proton with respect to $\vec{q}$, in the cm-frame. Note that the angles ϕ_{np} and θ_{np} are closely related to the missing momentum. A large tensor asymmetry is expected for perpendicular kinematics with $\phi_{np} = 180°$ and $p_m \perp \vec{q}$. If the deuteron spin is perpendicular to the momentum transfer, then the asymmetry is predicted to be negative and its magnitude is expected to increase with θ_{np} (or p_m) due to the D-state contributions to the deuteron ground-state wave function [4]. Fig. 1a shows the tensor asymmetry obtained as a function of θ_{np} for protons in a ϕ_{np}-range between 150° and 210° and with a kinetic energy larger than 40 MeV. The spin was aligned perpendicular to the momentum transfer and oriented in the scattering plane. Data are compared to the results of the PWBA (dashed curve) and the full (solid curve) calculation of Arenhövel *et al.* [4] using a Monte Carlo to average over the kinematic region.

By orienting the spin parallel to the momentum transfer, the asymmetry is expected to change sign. The obtained data shown in Fig. 1b follow this prediction. However, the data deviate from the results of a PWBA calculation. The calculation which includes contributions from FSI, MEC and IC, and relativistic corrections gives a better description of the data. Assuming that in

the present kinematics FSI is the dominant contribution, the difference between the results of the two calculations can be related to the spin-dependence of the final-state interaction. The data show that, when the deuteron spin is aligned parallel with respect to the momentum transfer, the struck proton more strongly interacts with the neutron [5].

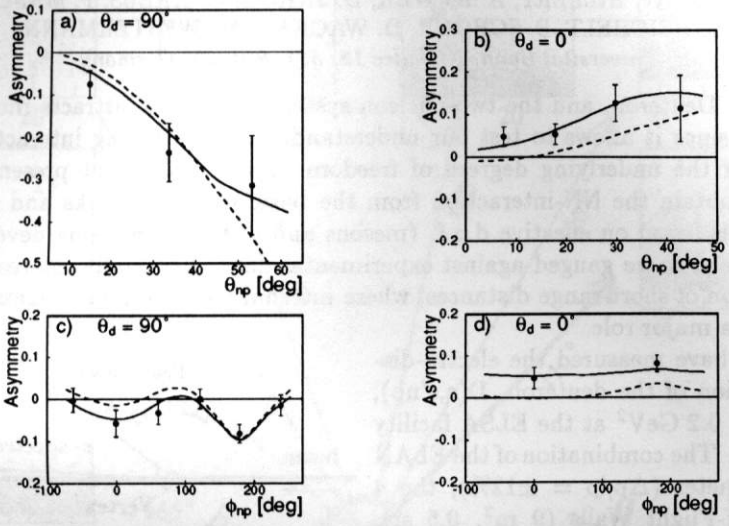

Figure 1: Tensor asymmetries as functions of θ_{np} and ϕ_{np} for the spin parallel and perpendicular to the momentum transfer. Data are compared to the results of a PWBA (dashed curve) and a full (solid curve) calculation of Arenhövel et al. [4].

We plan to pursue measurements with higher luminosities to yield data for missing-momenta around 300 MeV/c [6].

This work was supported in part by the Nederlandse Organisatie voor Wetenschappelijk Onderzoek, the Swiss National Foundation, the National Science Foundation under Grants No. PHY-9316221 (UW), PHY-9200435 (ASU) and HRD-9154080 (Hampton), NATO Grant No. CRG920219.

1. Three contributions to this conference by M. Bouwhuis, J.F.J. van den Brand and M. Ferro-luzzi.
2. E. Passchier *et al.*, to be submitted to *Nucl. Instrum. Methods* A, (1996).
3. Z.-L. Zhou, M. Ferro-Luzzi, J.F.J. van den Brand, H.J. Bulten *et al.*, accepted for publication by *Nucl. Instrum. Methods* A, (May, 1996).
4. H. Arenhövel *et al.*, *Phys. Rev.* C **46**, 455 (1992).
5. S. Jeschonnek *et al.*, contribution to this conference.
6. J.L. Forest, V.R. Pandharipande *et al.*, UIUC-preprint 96-03-022.

STUDY OF THE EXCLUSIVE *ed*-SCATTERING AT VEPP-3

A.V.Osipov, A.A.Sidorov, V.N.Stibunov
INP, Tomsk, Russia

D.M.Nikolenko, S.G.Popov, I.A.Rachek, D.K.Toporkov
BINP, Novosibirsk, Russia

E.I.Tsentalovich
BINP, present address: MIT Bates, MA, USA

B.B.Wojtsekhowski
BINP, present address: CEBAF, Newport News, VA, USA

We report here the experimental values of the cross section and the target tensor asymmetry in the electro production of the two protons from the tensor polarized deuteron by 2 GeV electrons in a channel with undetected pion.

The data were collected in parallel with the experiments performed by collaboration Novosibirsk, Argonne, Amsterdam, St. Petersburg, Tomsk, which used an internal tensor-polarized deuterium target in the VEPP-3 electron storage ring [1,2]. By using $\vec{d}(e,pp)\pi$ reaction we, for the first time, got the access to the region of large proton momenta in the polarized deuteron.

The data taking was performed at an average electron beam current of 150 mA. The total integral beam charge passed through the target was 386 kC. The target thickness $(3.05 \pm 0.12) \times 10^{11} atom/cm^2$ and the average value of the tensor target polarization $P_{zz} = 0.572 \pm 0.053$ were determined from the electron-deuteron elastic scattering [1].

The particle-detection apparatus [3] consists of two identical two-arm systems to detect the protons in coincidence. Each arm includes 6 drift chamber planes, three thin plastic scintillator counters (4, 10 and 10 mm thick) followed by a 20 cm thick plastic scintillator (top arms) or a 16 cm NaI(Tl) counter (bottom arms). Each proton arm detected particles within the range of angles $\theta = 68° - 82°$ and $\Delta\varphi = 40°$. The central azimuthal angles were 0° and 180° for one of the detection system, while 90° and 270° for the other one. The range of proton kinetic energy was 55 – 180 MeV for the top arms and 46 – 264 MeV for the bottom arms. Two procedures have been applied for calibration of the scintillation hodoscopes:

- measurements of the energy deposition in every layer by cosmic rays;
- data from $d(e,e'p)$ - and $d(e,pn)e'$ - reactions to determine the absolute energy scales.

Separation of protons from pions and deuterons was done by the $(E, dE/dx)$ method. The kinetic energy of the protons is reconstructed combining the values of the deposition in the detector layers. The UNIMOD code [4] was used to calculate the response of the scintillator layers. The resolution for the kinetic energy of the protons was determined to be 8% FWHM for low-energy protons and increased upto 12% FWHM for 260 MeV protons . The effective mass resolution of the *pp*-system was $4.2 - 8.1 MeV/c^2$ according to GEANT simulation. Several cuts were put on the data for background reduction:

- $68° \leq \theta^{lab}_{p_{1,2}} \leq 82°$;
- the proton vertexes in $\pm$ 0.7 *cm* from the beam line;
- the missing mass $M_x \geq m_\pi - \Delta M$ ($\Delta M = 5\ MeV/c^2$).

We selected 876 events for the two detector systems. The background from the walls of the storage cell was retained at the 6% level. For simulation of the $\vec{d}(e, pp)e'\pi^-$ experiment we designed the package NEWGAM. The data analysis has been performed in a nonrelativistic framework. The concept of a virtual photon has been used to relate the production negative pions by an electron scattering to the same proton-proton final state induced by the real photons. The virtual photon spectrum [5], upon integrating over electron scattering angles, has been used for the real photon spectrum, since contributions to that spectrum come predominantly from small scattering angles. One nucleon pion photoproduction operator has been taken from the Metcalf's and Wolker's phenomenological analysis[6]. The result presented in the Fig.1 was calculated with the deuteron wave function obtained by the Paris N-N potential [7].

For generation of events simulating the $d(e, pp)e'\pi^-$ reaction by Monte-Carlo method, the ENIGMA code[8] and the NEWGAM code, based on different theoretical models of the exclusive scattering process, were used. The package ENIGMA uses one nucleon pion photoproduction amplitude of Blomqvist-Laget[9]. By using all these simulating packages (UNIMOD, GEANT, ENIGMA and NEWGAM) we obtained:

- the mass-, momentum-, and angle resolution of the detector system;
- the effective angular acceptance, the efficiency of the detector arms and the counting rates;
- the energy deposition in the scintillation counters;
- all initial kinematic parameters for the accepted events.

The observed effective mass distribution of the *pp*-system is presented in Fig.1 together with the results of simulation by NEWGAM and ENIGMA. One can see a clear disagreement between the experimental data and the theoretical predictions both in shape and in absolute value.

The target asymmetry A_T was calculated from the difference in the count-

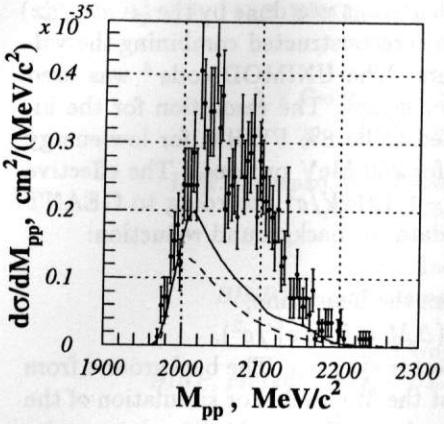

Figure 1: The cross section for $d(e,pp)e'\pi^-$ as function of the pp - system effective mass, integrated within the apparatus acceptance. Solid line – ENIGMA code, dashed line – NEWGAM code.

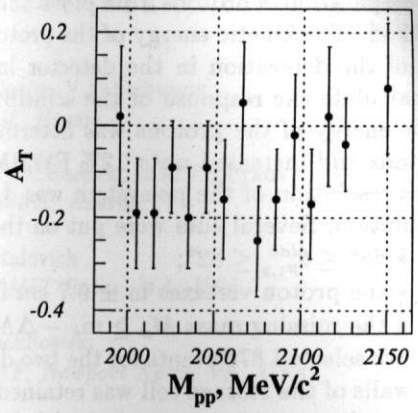

Figure 2: Experimental result for A_T as function of the pp - system effective mass.

ing rates for the opposite signs of P_{zz}. It is represented in Fig.2 as function of the pp - system effective mass. The corresponding region of the "slow" proton momenta is 300 – 550 Mev/c.

This work was supported by the Russian Fund of Fundamental Research under the contract 93-02-03514 and by the International Science Foundation under the contracts RI6000 and RI6300.

References

1. R.Gilman *et al*, *Phys. Rev. Lett.* **65**, 1733 (1990).
2. S.I.Mishnev *et al*, *Phys. Lett.* B **302**, 23 (1993).
3. L.G.Isaeva *et al*, *Nucl. Instrum. Methods* A **325**, 16 (1993).
4. A.D.Bukin *et al*, UNIMOD2. Preprint BINP 94-20, Novosibirsk, (1994).
5. R.H.Dalitz, D.R.Yennie, *Phys. Rev.* v **105**, 1598 (1957).
6. W.J.Metcalf, R.L.Walker, *Nucl. Phys.* B **76**, 253 (1974).
7. M.Lacombe *et al*, *Phys. Rev.* C **21**, 861 (1980).
8. J.L.Visschers, ENIGMA.: An event generator. Proc. of MC93 Int. Conf. on Monte Carlo Simulation in High Energy and Nucl. Phys. Ed.: P. Dragovitsch. World Scientific Publishing, (1994).
9. I.Blomqvist, J.M.Laget, *Nucl. Phys.* A **280**, 405 (1977).

FIRST EXCLUSIVE MEASUREMENT OF η PRODUCTION IN QUASIFREE PN COLLISIONS

R. BILGER[1], A. BONDAR[2], H. CALÉN[3], H. CLEMENT[1], C. EKSTRÖM[4], K. FRANSSON[3], L. GUSTAFSSON[3], S. HÄGGSTRÖM[3], B. HÖISTAD[3], A. JOHANSSON[3], T. JOHANSSON[3], K. KILIAN[5], S. KULLANDER[3], A. KUPSC[7], A. KUZMIN[2], P. MARCINIEWSKI[7], B. MOROSOV[6], J. MOEHN[3], A. MÖRTSELL[3], W. OELERT[5], A. POVTOREJKO[6], V. RENKEN[5], R. RUBER[3], U. SCHUBERTH[3], V. SIDOROV[2], B. SHWARTZ[2], J. STEPANIAK[7], A. SUKHANOV[2], A. SUKHANOV[6(3)], G.J. WAGNER[1], M. WATERS[5], Z. WILHELMI[8], J. ZABIEROWSKI[9], A. ZERNOV[6], J. ZLOMANCZUK[3]

[1] *Physicalisches Inst., Tübingen University, Germany;* [2] *BINP, Novosibirsk, Russia;* [3] *ISV, Uppsala University, Sweden;* [4] *TSL, Uppsala, Sweden;* [5] *IKP, KFA, Jülich, Germany;* [6] *JINR, Dubna, Russia;* [7] *INS, Warsaw, Poland;* [8] *Inst. of Exp. Phys., Warsaw University, Poland;* [9] *INS, Lodz, Poland*

Data on the total cross section of the quasifree reactions pp → ppη, pn → pnη and pn → dη for CM excess energies in the range of 15 - 115 MeV are presented.

The cross section for the reaction pp → ppη has been well measured from the threshold region up to a beam energy of 2 GeV by a number of experiments [1-4]. The η production in pn interactions is not as well known. The existing data indicate a much higher η-production cross section in pn-interactions than in pp-interactions. However these data either have large uncertainties [5] or are from inclusive measurements with a deuteron target [6] where only the η was detected.

In our experiment at the CELSIUS storage ring in Uppsala[7], η-production in pd-collisions has been studied using an internal cluster jet target and a proton beam at 1350 MeV. The detection of both the η, from the $\eta \rightarrow \gamma\gamma$ decay, and outgoing particles enables us to separate the different quasifree reaction channels, pp → ppη, pn → pnη and pn → dη. Due to the Fermi momentum of the target nucleons, the CM energy of the system consisting of the beam proton and target nucleon varies. Thus, for each η event, being consistent with one of the channels, the CM energy is reconstructed and the excitation functions can be extracted after correcting for the detector acceptance and the distribution of the Fermi momentum[8].

Our preliminary results on the quasifree cross sections for pp → ppη, pn → pnη and pn → dη are shown in Fig. 1. Phase space distributions have been assumed when calculating the detector acceptance and effects from *e.g.* nuclear shadowing and reabsorbtion of the η-meson have not yet been corrected

for. Only the statistical errors are indicated in the figure. The systematical errors are estimated to be of the order 30 %. Our excitation function for pp $\rightarrow$ ppη is in agreement with the previous measurements [1,2,4] within the systematical errors.

The cross section for pn $\rightarrow$ pnη is considerably larger than for pp $\rightarrow$ ppη but the shape is similar over the whole measured energy range (Fig. 2). The excitation function for pn $\rightarrow$ dη (shown separately in Fig. 3) is more flat and the shape is understood qualitatively by phase space and the excitation of the N*(1535) resonance [9] . The ratio between the pn $\rightarrow$ pnη and pn $\rightarrow$ dη cross sections is shown in Fig. 4. The curve is from a model of Fäldt and Wilkin [10] in which the the behaviour at low energy is shown to be dominated by the difference in the s-wave scattering state of the final NN system.

References

1. A. M. Bergdolt et al., *Phys.Rev.* **D48** (1993) R2969
2. E. Chiavassa et al., *Phys.Lett.* **B322** (1994) 270
3. E. Chiavassa et al., *Proc. of the sixth Int. Symposium on Meson-Nucleon Physics and the Structure of the Nucleon*, Blaubeuren/Tübingen, Germany, July 10-14, 1995, πN Newsletter, **10** (1995) 93
4. H. Calén et al., *Phys. Lett.* **B366** (1996) 39
5. E. Chiavassa et al., *Phys.Lett.* **B337** (1994) 192
6. F. Plouin, P. Fleury and C. Wilkin, *Phys. Rev. Lett.* **65** (1990) 690
7. H. Calén et al., *Detector setup for a cooler storage ring with internal target*, to appear in Nucl. Instr. Meth.
8. M. Lacombe et al., *Phys. Lett.* **B101** (1981) 139
9. G. Fäldt and C. Wilkin, private communication
10. G. Fäldt and C. Wilkin, *TSL/ISV-95-0127* December 1995

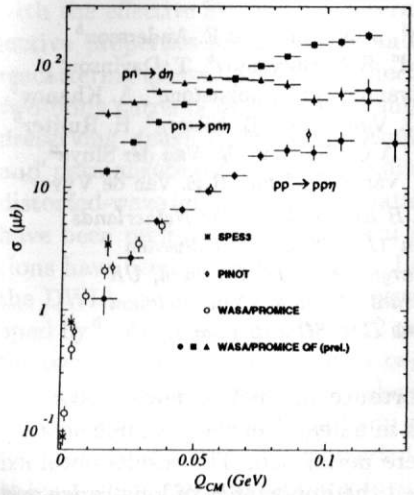

Figure 1: Cross sections for the reactions $pp \to pp\eta$, $pn \to pn\eta$ and $pn \to d\eta$ as a function of the excess energy in the centre of mass system of the final state.

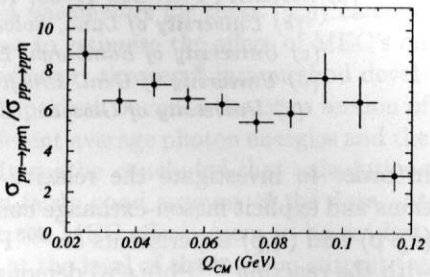

Figure 2: Cross section ratio between the reactions $pn \to pn\eta$ and $pp \to pp\eta$.

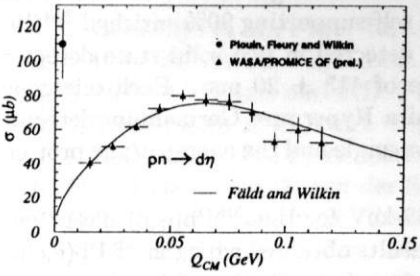

Figure 3: Cross section for the reaction $pn \to d\eta$.

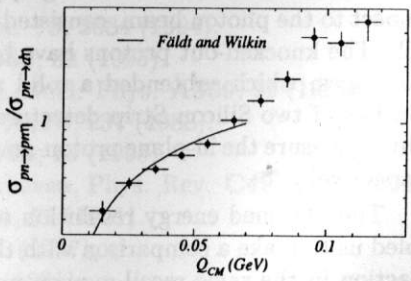

Figure 4: Cross section ratio between the reactions $pn \to pn\eta$ and $pn \to d\eta$.

CELSIUS AS AN η FACTORY

R. BILGER[14], M. BLOM[6], D. BOGOSLAWSKY[8], A. BONDAR[4], W. BRODOWSKI[14], H. CALÉN[6], B. CHERNYSHEV[11], I. CHUVILO[7], H. CLEMENT[14], S. DAHLGREN[6], V. DUNIN[8], C. EKSTRÖM[13], C.-J. FRIDÉN[13], K. FRANSSON[6], M. GORNOV[11], Y. GUROV[11], L. GUSTAFSSON[6], H. HIRABAYASHI[9], S. HÄGGSTRÖM[6], B. HÖISTAD[6], H. IKEGAMI[12], A. JANSSON[6], A.JOHANSSON[6], T. JOHANSSON[6], K. KILIAN[10], G. KOLACHEV[4], M. KOMOGOROV[8], L. KOMOGOROVA[8], S. KULLANDER[6], A. KUPSC[2], A. KUZMIN[4], A. KUZNETSOV[8], P. MARCINIEWSKI[2], A. MARTEMYANOV[7], Y. MIZUNO[12], B. MOROSOV[8], J. MOEHN[6], A. NAWROT[2], W. OELERT[10], Z. PAWLOWSKI[5], A. POVTOREJKO[8], T. PURLATZ[4], D. REISTAD[13], R. RUBER[6], S. SANDUKOVSKY[8], R. SHAFIGULLIN[11], B. SHWARTZ[4], V. SIDOROV[4], V. SOPOV[7], J. STEPANIAK[2], A. SUKHANOV[4], A. SUKHANOV[8(6)], V. TCHERNYSHEV[7], V. TIKHOMIROV[8], A. TUROWIECKI[1], G. WAGNER[14], Z. WILHELMI[1], A. YAMAMOTO[9], A. YAMAOKA[9], Y. YUASA[12], J. ZABIEROWSKI[3], A. ZERNOV[8], J. ZLOMANCZUK[1(6)]

[1] IEP, Warsaw University, Poland; [2] INS, Warsaw, Poland; [3] INS, Lodz, Poland; [4] BINP, Novosibirsk, Russia; [5] IRE, Warsaw Technical University, Poland; [6] ISV, Uppsala University, Sweden; [7] ITEP, Moscow, Russia; [8] JINR, Dubna, Russia; [9] KEK, Tsukuba, Japan; [10] KFA, Jülich, Germany; [11] MEPI, Moscow, Russia; [12] RCNP, Osaka, Japan; [13] TSL, Uppsala, Sweden; [14] Tübingen University, Germany

The rare decays of the η meson are of great interest for investigations of P, C and CP symmetries and for tests of chiral pertubation theory in strong and electromagnetic interactions. The η meson has unique properties and is well suited for such studies: high mass, small mass width and the quantum numbers as those of the vacuum. High-precision experiments on rare decays of light mesons are currently being prepared within the WASA project - a high-luminosity experiment using a close to 4π detector configuration[1, 2] at the CELSIUS ion storage ring at the The Svedberg Laboratory, Uppsala.

The CELSIUS ring[2] is a combined accelerator and storage ring with a circumference of 81.8 m. The ring consists of four 90^0 magnet quadrants and four straight sections. The latter are used for injection of the ions from the Gustaf Werner cyclotron, electron cooling, and experiments at two target stations with a cluster-jet[3] and a pellet target[4], respectively. The beams in CELSIUS range from protons to argon ions with maximum energies of 1360 MeV for protons and 470 MeV/u for ions with charge-to-mass ratio of 1/2. An application for funds has been submitted to increase the magnetic field by 30% in order to reach 9 Tm.

The target system to be used in the WASA experiments has to fulfil a number of strong requirements; a target thickness about 20 times that of the cluster-jet target[3], a target beam travelling abot 2 m in a narrow tube through the central detector, a good vertex definition and minimum pertubation to the stored beam and to the ring vacuum. To fulfil these requirements, a pellet target generator providing a stream of frozen hydrogen microspheres has been proposed[5] and developed[6].

The production of the pellets by breaking up a liquid jet into droplets at triple point conditions and the injection into vacuum is described in detail in Ref. 6. The pellets of 40 μm diameter, later reduced to 30 μm by using a more narrow injection nozzle, have a speed of 60 m/s and a total flow of about $7x10^4$ per second. The pellet stream moves with an angular divergence of ±0.04° about 4 meters before being trapped in a cryogenic beam dump. The pellets have been exposed to 200, 310 and 900 MeV protons and 570 MeV deu-terons circulating in the CELSIUS ring. The results from the test experiments[4] show that an optimal target thickness of $5x10^{15}$ atoms/cm^2 will give acceptable lifetimes of the circulating ion beam, a few minutes at energies around 1 GeV, as well as acceptable vacuum conditions, about 10^{-6} mbar, in the scattering chamber. All major requirements on the target system to be used in the WASA experiments have been shown to be fulfilled by the hydrogen pellet target. Future developments include the diagnostics for the pellet tracking, and the production of deuterium pellets.

The WASA experimental setup includes the pellet-target system described above, a central detector for particles scattered isotropically, a forward detector for particles scattered at angles below 18°, and a tagging spectrometer located in the magnet quadrant following the WASA setup for He recoils emitted at 0°. The main emphasis of the WASA experimental programme is put on the decay channels of the η meson. The CELSIUS ring with the pellet target will serve as an efficient η factory producing about $3x10^7$ η mesons per day at a luminosity of 10^{32} cm^{-2}s^{-1} and a duty factor of 75%. A positive outcome of the developments of deuterium pellets will increase the production rate a factor of 5.

1. S. Kullander (spokesman), *WASA: Wide Angle Shower Apparatus for Particle Physics at CELSIUS*, Proposal 1987.
2. *TSL Progress Report 1994-1995*, ed. A. Ingemarsson, The Svedberg Laboratory, Box 533, S-751 21 Uppsala, Sweden.
3. C. Ekström, *Internal Targets at the CELSIUS Storage Ring*, Proc. 19th INS Int. Symp. on Cooler Rings and their Application, Tokyo, Japan, 1990, p. 228.
4. C. Ekström et al., *Nucl. Instr. and Meth. in Phys. Res.* A371(1996)572.
5. S. Kullander, *CELSIUS information day*, 1984-10-01.
6. B. Trostell, *Nucl. Instr. and Meth. in Phys. Res.* A362(1995)41.